JOURNAL OF THE KOREAN ASTRONOMICAL SOCIETY
33: 111 ~ 121, 2000

FORMATION OF PROTO-GLOBULAR CLUSTER CLOUDS BY THERMAL INSTABILITY

HYESUNG KANG[1], GEORGE LAKE[2], AND DONGSU RYU[3]
[1]Department of Earth Sciences, Pusan National University, Pusan 609-735, Korea
[2]Department of Astronomy, University of Washington, Box 351580, Seattle, WA 98185-1580, USA
[3]Department of Astronomy & Space Science, Chungnam National University, Daejeon 305-764, Korea
E-mail: kang@uju.es.pusan.ac.kr, lake@heremes.astro.washington.edu, and ryu@canopus.chungnam.ac.kr
(Received Aug. 7, 2000; Accepted Sep. 19, 2000)

ABSTRACT

Many models of globular cluster formation assume the presence of cold dense clouds in early universe. Here we re-examine the Fall & Rees (1985) model for formation of proto-globular cluster clouds (PGCCs) via thermal instabilities in a protogalactic halo. We first argue, based on the previous study of two-dimensional numerical simulations of thermally unstable clouds in a stratified halo of galaxy clusters by Real *et al.* (1991), that under the protogalactic environments only nonlinear ($\delta \gtrsim 1$) density inhomogeneities can condense into PGCCs without being disrupted by the buoyancy-driven dynamical instabilities. We then carry out numerical simulations of the collapse of overdense clouds in one-dimensional spherical geometry, including self-gravity and radiative cooling down to $T = 10^4$ K. Since imprinting of Jeans mass at 10^4 K is essential to this model, here we focus on the cases where external UV background radiation prevents the formation of H_2 molecules and so prevent the cloud from cooling below 10^4 K. The quantitative results from these simulations can be summarized as follows: 1) Perturbations smaller than $M_{\rm min} \sim (10^{5.6}\ {\rm M}_\odot)(n_h/0.05\ {\rm cm}^{-3})^{-2}$ cool *isobarically*, where n_h is the unperturbed halo density, while perturbations larger than $M_{\rm max} \sim (10^8\ {\rm M}_\odot)(n_h/0.05\ {\rm cm}^{-3})^{-2}$ cool *isochorically* and thermal instabilities do not operate. On the other hand, intermediate size perturbations ($M_{\rm min} < M_{\rm pgcc} < M_{\rm max}$) are compressed *supersonically*, accompanied by strong accretion shocks. 2) For supersonically collapsing clouds, the density compression factor after they cool to $T_c = 10^4$ K range $10^{2.5} - 10^6$, while the isobaric compression factor is only $10^{2.5}$. 3) Isobarically collapsed clouds ($M < M_{\rm min}$) are too small to be gravitationally bound. For supersonically collapsing clouds, however, the Jeans mass can be reduced to as small as $10^{5.5}\ {\rm M}_\odot(n_h/0.05\ {\rm cm}^{-3})^{-1/2}$ at the maximum compression owing to the increased density compression. 4) The density profile of simulated PGCCs can be approximated by a constant core with a halo of $\rho \propto r^{-2}$ rather than a singular isothermal sphere.

Key words : galaxy : globular clusters : general – hydrodynamics – instabilities

I. INTRODUCTION

Globular clusters (GCs) are the oldest relics in our galaxy, presenting a cosmological challenge, as their ages often burst the allowed bounds of the expansion age. Since there are *at least* three distinct populations of GCs, the old halo and the middle-aged disk populations of GCs in our Galaxy (Zinn 1985), and the young GCs in interacting galaxies (Ashman & Zepf 1992), we may well need more than one model to explain their formation and evolution. In the present study, we focus on the formation of the halo GCs. Half of the total mass of our galaxy appears to be contained within ~ 50 kpc, whereas roughly half of the luminosity of the disk as well as half of the total number of halo GCs are distributed within the solar galactocentric distance (~ 8 kpc). So halo GCs clearly know about the *dissipation* that followed galaxy formation and we must place their formation in the protogalactic context. This encourages models that form halo clusters during the formation of the protogalaxy, such as thermal instabilities in the protogalactic halo (Fall & Rees 1985) or pregalactic cloud collisions (Gunn 1980; Lake 1987; Kang *et al.* 1990; Kumai, Basu, & Fujimoto 1993).

Many models of globular cluster formation assume the presence of *proto-globular cluster clouds* (PGCCs) in pressure equilibrium with hot halo gas (*e.g.,* Gunn 1980; Dopita & Smith 1986; Brown, Burkert & Truran 1991; Kumai, Batsu, & Fujimoto 1993). The model by Fall & Rees (1985, FR85 hereafter) has been most widely adopted to explain the formation of such PGCCs: the thermal instability drives catastrophic cooling of over-dense regions in the hot halos of protogalaxies and condenses them to dense clouds. In the present study, adopting FR85 model, we follow the thermal and dynamical evolution of over-dense clouds by numerical simulations in order to examine more quantitatively the physical properties of resulting PGCCs.

Although the thermal instability was extensively investigated in several areas of astrophysics, in recent years it has received much attention especially for X-

ray cluster cooling flows: (*cf.* Balbus 1986; Malagoli, Rosner & Bodo 1987; Balbus & Soker 1989; Malagoli, Rosner, & Fryxell 1990). According to the results from numerical simulations in one-dimensional (1D) geometries (David, Bregman & Seab 1988 [DBS88 hereafter]; Brinkmann, Massaglia & Müller 1990 [BMM90]), the over-density undergoes a *quasi-static compression* in near pressure equilibrium when a cloud is small enough to adjust to pressure change faster than it cools, while larger clouds may undergo a "supersonic compression stage", leading to a density increase much higher than what is expected from the isobaric compression. The plane-parallel calculations by DBS88 showed that the density contrast increases to the "isobaric" ratio of the temperature of the hot background medium ($T_h \sim 10^7 - 10^8$ K) and the minimum temperature ($T_c \sim 10^4$ K) where the cooling becomes inefficient. On the other hand, the spherically symmetric calculations of BMM90 showed that the density contrasts can be more than three orders of magnitude higher than those found in the plane-parallel calculations of DBS88. The difference between two geometries is mainly due to the fact that the gravitational acceleration increases as GM/R^2 when the spherical cloud collapses, while it remains the same (independent of R) when the plane sheet compresses. Also isotropic spherical compression (focusing) leads to much higher density accelerating the cooling and rise in density. However, 2D simulations of the collapse of an elongated blob by BMM90 showed a shape instability to a pancake-shape leading to evolution best represented by the 1D plane-parallel case. Thus geometry is clearly important in the nonlinear evolution. On the other hand, 2D simulations by Vázquez-Semadeni, Gazol, & Scalo (2000) showed that the condensation of fluctuating density field via thermal instability leads to a network of transient filaments which later accrete onto isolated round blobs. These blobs form at intersections between filaments just like galaxy clusters in large-scale structure formation in cosmological simulations. This implies that the 1D spherical simulation can actually represent a generic collapse of the highest density peaks in the randomly fluctuating density field in 3D.

Numerical simulations in a 2D stratified background (Yoshida, Hattori, & Habe 1991; Reale *et al.* 1991 and references therein), on the other hand, have shown that the dynamic instabilities, such as Rayleigh-Taylor and Kevin-Helmholtz instabilities due to buoyancy-driven oscillations can disrupt the thermally unstable bubbles if the timescale for buoyancy oscillation (Brunt-Väsälä period) is shorter than the local radiative cooling time. Thus it is believed that the classic theory of thermal instability can not explain the effective mass depletion from the cooling flows of galactic clusters. We will examine the role of such dynamic instabilities for the formation of PGCCs in the protogalactic halo environment in the next section. The details of our models are given also in this section. The main results are in Section III. Conclusions are given in Section IV.

II. MODEL CALCULATIONS

(a) Protogalactic Halo Model

We adopt an idealized model for the protogalactic halo gas as in FR85; an isothermal sphere based on the Milky Way's properties, with a circular velocity $V_c = 220$ km s^{-1} and corresponding gas temperature $T_h = 1.7 \times 10^6$ K.

Many previous studies used a gas distribution specified by the condition that the free fall time to the center of the protogalaxy equals the cooling time, yielding the halo gas density at a distance R_g from the center $\rho_1 \sim 1.7 \times 10^{-25}$ g cm$^{-3}(R_g/10$ kpc$)^{-1}$. The use of ρ_1 has lead previous workers to consider halo densities of $n_h = 0.1$ cm^{-3} (FR85; Kang *et al.* 1990) or even $n_h = 1$ cm^{-3} (Vietri & Pesce 1995). For a primordial gas of H and He with an assumed ratio $n(\mathrm{He})/n(\mathrm{H}) = 0.1$, the halo gas mass density is $\rho_h = (2.34 \times 10^{-24}$ g cm$^{-3})n_h$. For the isothermal sphere in hydrostatic equilibrium, however, the gas density is given by $\rho_2 = 5.8 \times 10^{-25}$ g cm$^{-3} f_B (R_g/10$ kpc$)^{-2}$, where f_B is the ratio of the baryonic to total matter density. Realistic values should be $0.02 \lesssim n_h \lesssim 0.07$ cm^{-3} for $R_g \sim 10$ kpc (assuming $f_B \sim 0.1$) with some degree of central concentration. A value as high as $n_h = 1$ cm^{-3} is greater than the total density of baryonic and dark matter. Thus we take 0.05 cm^{-3} as a fiducial value and express the halo gas density as

$$n_h \approx (0.05 \text{ cm}^{-3}) R_{10}^{-q}, \tag{1}$$

where R_{10} is R_g in units of 10 kpc and $1 \lesssim q \lesssim 2$.

Although the density irregularities in protogalaxies likely result from a superposed spectrum of perturbations, we consider, for simplicity, isolated spherically symmetric clouds resulted from sinusoidal perturbations. So the initial gas density of the cloud n_{cloud} decreases gradually with radius r from its center to its edge R_c as follows:

$$n_{cloud} = n_h \left[1.0 + \delta \cos\left(\frac{\pi}{2}\frac{r}{R_c}\right)\right] \quad \text{for } r < R_c \tag{2}$$

where δ is the amplitude of the initial density perturbation and R_c is the cloud radius.

The initial temperature throughout the cloud is set by the condition of hydrostatic equilibrium. To start in the nearly linear regime, we always begin with $\delta \sim 1$, unless otherwise noted. Initial parameters of the model clouds are summarized in Table 1.

(b) Time Scales

The free fall time t_{ff}^{pg} is the time it takes a particle dropped from R_g to reach the center of the protogalaxy,

$$t_{ff}^{pg} = \left(\frac{\pi}{2}\right)\left(\frac{R_g}{V_c}\right) = 5.6 \times 10^7 \text{ yrs}\left(\frac{R_g}{10 \text{ kpc}}\right) \tag{3}$$

Table 1. Initial Parameters for Model Clouds

Model	n_h (cm^{-3})	δ	R_c/l_{cool} [a]	R_c (pc)	M_c ($M_\odot$)	flow motion[b]
SM1	0.1	1	0.042	4.20×10^1	1.4×10^3	isobaric
SM2	0.1	1	0.092	9.24×10^1	1.5×10^4	isobaric
SM3	0.1	1	0.21	2.10×10^2	1.8×10^5	isobaric
SM4	0.1	1	0.42	4.20×10^2	1.4×10^6	supersonic
SM5	0.1	1	0.63	6.30×10^2	4.9×10^6	supersonic
SM6	0.1	1	1.1	1.05×10^3	2.3×10^7	supersonic
SM7	0.1	1	2.1	2.10×10^3	1.8×10^8	isochoric
SM8	0.1	5	2.1	2.10×10^3	3.2×10^8	isochoric
SM9	0.1	0.5	0.42	4.20×10^2	1.3×10^6	isochoric
SM11	1.0	1	0.17	1.71×10^1	9.8×10^2	isobaric
SM12	1.0	1	0.42	4.22×10^1	1.4×10^4	supersonic
SM13	1.0	1	0.68	6.83×10^1	6.2×10^4	supersonic
SM14	1.0	1	1.4	1.37×10^2	4.9×10^5	supersonic
SM15	1.0	1	2.7	2.73×10^2	4.0×10^6	isochoric
SM16	1.0	1	5.5	5.46×10^2	3.2×10^7	isochoric
SM21	0.01	1	0.10	1.02×10^3	2.1×10^6	isobaric
SM22	0.01	1	0.12	1.23×10^3	8.6×10^6	isobaric
SM23	0.01	1	0.21	2.05×10^3	1.7×10^7	supersonic
SM24	0.01	1	0.33	3.28×10^3	6.9×10^7	supersonic
SM25	0.01	1	0.41	4.10×10^3	1.3×10^8	supersonic
SM26	0.01	1	0.61	6.14×10^3	4.5×10^8	supersonic
SM27	0.01	1	0.82	8.19×10^3	1.1×10^9	isochoric

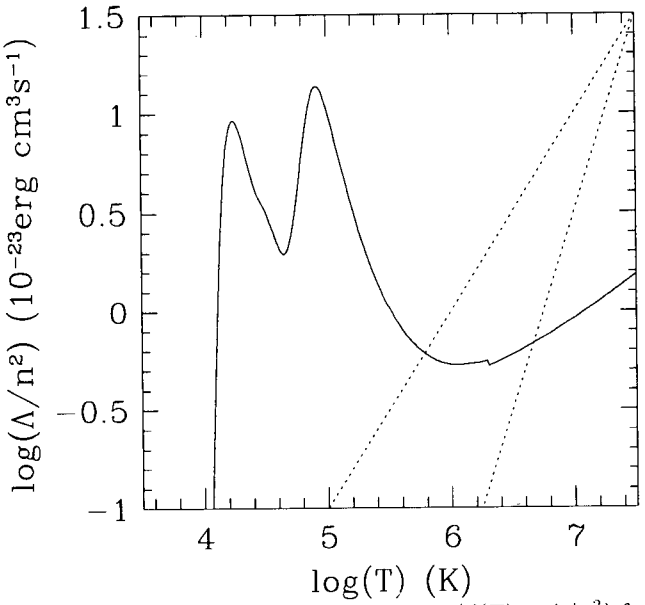

Fig. 1.— The equilibrium cooling rate ($f(T) = \Lambda/n^2$) for a primordial gas composed of H and He is given in units of 10^{-23}erg cm^3 s^{-1}. Dotted lines show $d\ln(\Lambda/n^2)/d\ln T = 1$ and $d\ln(\Lambda/n^2)/d\ln T = 2$.

The free fall time of a uniform gas cloud including only its self-gravity is

$$t_{ff}^{sg} = \left(\frac{3\pi}{32G\rho}\right)^{1/2} = 4.4\times10^6 \text{ yrs}\left(\frac{n}{100 \text{ cm}^{-3}}\right)^{-1/2}, \quad (4)$$

where n is the cloud density and any dark matter contribution is ignored.

The cooling time for the halo gas of T_h is given by

$$t_{cl,h} = \frac{1.5 n_h k T_h}{\Lambda} \approx (4.0\times10^7 \text{ yrs}) R_{10}^q, \quad (5)$$

where the cooling rate of $\Lambda/n_h^2 = 5.5\times10^{-24}$erg cm^{3}s^{-1} at $T_h = 1.7\times10^6$ and the halo density given in Eq. (1) are used to calculate the latter relation. For an *isobaric* perturbation of the density contrast δ, the cooling timescale of the perturbed gas becomes $t_{cl,c} \approx t_{cl,h}(1+\delta)^{-2}$, considering that the cooling rate is almost constant for temperatures within factor of two of $T \sim 10^6$ K. We define the *cooling distance* as the distance over which the sound wave of the hot gas can travel within the cooling timescale of the perturbed gas,

$$l_{cool} \approx c_h t_{cl,c} \approx (8.1\times10^3 \text{ pc}) R_{10}^q (1+\delta)^{-2} \quad (6)$$

where $c_h = 198$ km s^{-1} is the sound speed of the hot gas of T_h.

The ratio of the cooling time to the self-gravity time for initial clouds is

$$\eta = 6.2 \times 10^{-2} R_{10}^{q/2} \left(\frac{1+\delta}{2}\right)^{-3/2} \quad (7)$$

For the range of density considered here, $0.01 < n_h < 1$ cm^{-3}, cooling takes place too fast for self-gravity to be important initially. However, the cooling becomes inefficient once the gas cools to 10^4K, and the gravitational time scale decreases as the density increases. The density in the condensed clouds increases by a factor of $\chi_{isob} = (T_h/T_c)(\mu_c/\mu_h) \sim 350$ for an isobaric case, where μ_c and μ_h are the molecular weights of the cold and hot gas, respectively. The density enhancement is even higher for supersonic collapses, resulting in the cloud pressure higher than the background pressure. The typical additional enhancement in supersonic collapses is $10^2 - 10^{3.5}$ (see the next section). Thus, self-gravity becomes dynamically important in late stages. Also note that self-gravity would be more important for lower density environments, since $\eta \propto n_h^{-1/2}$.

The growth of thermal instabilities in a stratified medium is affected by the buoyancy-driven dynamical instabilities (see below), so the local buoyancy oscillation period is also important. For our halo model it can be estimated by the local scale height H divided by the sound speed c_h,

$$t_b \sim \frac{H}{c_h} \sim (5.0 \times 10^7 \text{ yrs}) R_{10}, \quad (8)$$

since $H \sim R_g$ for the power-law density distribution assumed here. For linear initial perturbation (*e.g.*, $\delta << 1$), the cooling time is about the same as the buoyancy oscillation period ($t_{cl,c} \sim t_b$) and the cooling distance is about the size of scale height of the halo ($l_{cool} \sim R_g$). This means the global stability needs to be considered (Balbus & Soker 1989) for such perturbations.

(c) Effects of Dynamical Instabilities

When a bubble-shaped perturbation condenses due to radiative cooling, it falls along the direction of gravity and so it is subject to the Rayleigh-Taylor and Kevin-Helmholtz instabilities. Nonlinear evolution of such perturbations in a stratified halo of X-ray clusters was followed via numerical simulations (Hattori & Habe 1990; Yoshida, Hattori, & Habe 1991; Reale *et al.* 1991). The bubble is disrupted by these instabilities on a buoyancy oscillation period if it does not cool and condense significantly. Thus the cooling timescale must be shorter than the buoyancy oscillation period in order to prevent the disruption of the bubble. That depends on three parameters in order of importance: the ratio of the local buoyancy oscillation period to the local cooling time, the initial density contrast of the perturbation, and the ratio of the perturbation radius to the local scale-height (Reale *et al.* 1991). We note here the first and second parameters are not completely independent, since the cooling time of the perturbed gas is dependent on the initial density contrast.

Following Reale *et al.* (1991), we define for our protogalactic halo model,

$$\xi = \frac{t_b}{t_{cl,c}} \sim 1.25(1+\delta)^2 R_{10}^{(1-q)}, \quad (9)$$

using Eq. (6). According to their 2D numerical simulations, for $\xi \approx 1$ the perturbations lead to fragmentation due to the dynamical instabilities, but the fragments can be thermally unstable. For $\xi \gtrsim 5$, the perturbation cools and condenses so rapidly that the dynamical instabilities do not have time to disrupt the bubble. These numerical simulations find that thermal instabilities cannot be an effective mechanism for mass depletion from the X-ray cluster cooling flows, since typically $\xi \sim 0.01$ there. According to Eq. (9), on the other hand, $\xi \sim 5$ for $\delta \sim 1$ in a protogalactic halo, so the galactic halo provides more favorable conditions for thermal instabilities.

Thus the initial density contrast of the perturbations is the next important physical parameter. Here, we will take the generic view that the protogalaxy was formed from the hierarchical clustering of smaller substructures and contains some clumpiness and turbulences. We suggest only *nonlinear* (*i.e.* $\delta \gtrsim 1$) inhomogeneities in the protogalactic halo can condense due to thermal instabilities without being disrupted by the buoyancy-driven dynamical instabilities.

(d) Numerical Method

The gas dynamical equations including self-gravity and cooling are:

$$\frac{d\rho}{dt} + \rho \nabla u = 0, \quad (10)$$

$$\frac{du}{dt} = -\frac{1}{\rho}\nabla P + g, \quad (11)$$

$$\frac{de}{dt} = -\frac{1}{\rho}\nabla(Pu) + gu - \frac{\Lambda}{\rho}, \quad (12)$$

where $e = (\gamma - 1)p/\rho + (1/2)u^2$ is the total energy of the gas per unit mass and g is the gravitational acceleration. We use the Piecewise Parabolic Method (PPM) (Colella & Woodward 1984) in one-dimensional spherical geometry and treat gravity and cooling as source terms. The gravitational acceleration is softened near the center according to

$$g = -\frac{GM(<r)}{[\max(r,s)]^2}, \quad (13)$$

where G is the gravitational constant, $M(<r)$ is the mass within the radius r, and $s \sim 0.04R_c$ is the softening length. In most previous numerical simulations of the thermal instability (*e.g.*, , the references in §1),

self-gravity was ignored because the gravitational time scale was longer than the cooling time scale and/or the emphasis was on the effects of the thermal instability alone. In our models, the gravitational time scale is longer than the cooling time scale initially, but not at later times. Thus, we must follow the transition of the inward flow from being driven by background pressure at early times to self-gravity in the last stages of collapse.

The simulations start at $t = 0$ with the clouds at rest in pressure equilibrium and cease when the *background* gas has cooled to 10^4 K (see below). The standard mirror condition for the reflecting boundary at the center is used, while the flow is assumed to be continuous across the outer boundary.

(e) Radiative Cooling Rate

Our radiative cooling rate $f(T)$ applies to a primordial gas in ionization equilibrium (*cf.* Shapiro & Kang 1987). (The cooling rate per unit volume $\Lambda = n^2 f(T)$ where $f(T)$ is a function of temperature only.) The success of FR85 model is hinged on *imprinting* of the gravitationally unstable mass scale of PGCCs at 10^4 K which is similar to the characteristic mass scale of GCs. This requires that formation of H_2 molecules should be delayed longer than a free fall time of PGCCs. Kang *et al.* (1990) suggested that the globular cluster might have formed only during the phase when the protogalaxies are bright in UV background radiation. Hence we assume a model in which UV background radiation prevents formation of H_2 , so that the cooling rate is zero below 10^4 K and the minimum temperature is set at 10^4 K.

The criterion for the thermal instability is that the over-density continues to cool faster than its surroundings, requiring $d\ln f(T)/d\ln T < 1$ to destabilize isochoric condensations and $d\ln f(T)/d\ln T < 2$ to destabilize isobaric condensations (Balbus 1986). Fig. 1 shows $f(T)$ and includes dotted lines where $d\ln f(T)/d\ln T = 1$ and $d\ln f(T)/d\ln T = 2$.

We ignore the poorly understood process of thermal conduction. With the classical Spitzer (1979) conductivity, thermal conduction may dominate over the cooling. If we assume that the heat flux is *saturated* when the particle mean free path is comparable to the length scale of the temperature variation, the conductivity is one or two orders of magnitude smaller than the Spitzer value (see Gray & Kilkenny 1980). Brinkmann, Massaglia & Müller (1990) showed that flow quantities differ $\lesssim$3% when they added the reduced thermal conduction to their simulations of hot gas in clusters of galaxies.

III. SIMULATION RESULTS

(a) Classification by Cloud Size

We calculated spherical collapses for a wide range of halo densities ($0.01\ \mathrm{cm}^{-3} \leq n_h \leq 1\ \mathrm{cm}^{-3}$) and cloud sizes ($0.04 \lesssim R_c/l_{cool} \lesssim 2.5$). Initial parameters of the model clouds are summarized in Table 1, where M_c is the mass of the cloud contained within the initial perturbation.

Radiative cooling of the cloud leads to three different types of flow motions depending on its size relative to the cooling distance, as recognized in previous studies (FR85, DBS88). According to our simulations, they can be summarized as follows: 1) $(R_c/l_{cool}) \lesssim 0.2$, *small* isobaric compression regime, 2) $0.2 \lesssim (R_c/l_{cool}) \lesssim 1 - 1.5$, *intermediate* supersonic compression regime, and 3) $(R_c/l_{cool}) \gtrsim 1 - 1.5$, *large* isochoric cooling regime. While in *small* clouds the collapse remains isobaric and quasi-static, in *large* clouds the central gas cools almost isochorically and the thermal instability fails. Examples of these limiting cases are plotted in Fig. 2. Spherical collapses of clouds with $R_c/l_{cool} \sim 0.04$ and $R_c/l_{cool} \sim 2$ in the background halo with $n_h = 0.1\ \mathrm{cm}^{-3}$ and $T_h = 1.7 \times 10^6$ K are shown. Although the transitions between types are obviously continuous and gradual, we classified our models into "isobaric", "supersonic", and "isochoric" types according to the characteristics of flow motions in the simulations. The last column of Table 1 shows the types.

The *intermediate* size clouds belong to the most interesting regime. In order to see the evolution of an intermediate size cloud and the geometrical effects, spherical collapse as well as plane-parallel collapse were calculated for one model: $T_h = 1.7 \times 10^6$ K, $n_h = 0.1\ \mathrm{cm}^{-3}$, $l_{cool} \approx 10^3$ pc, and the scale height of the plane slab, H, and the radius of the cloud, R_c, are $H = R_c = 410\ \mathrm{pc} \sim 0.4 l_{cool}$. Fig. 3 shows the evolution at $t/t_{cl,c} = 1.3, 1.5, 1.7, 1.9$, and 2.2, where $t_{cl,c} = 5.0 \times 10^6$ yrs. In both geometries, the gas cools isobarically until $T \sim 2.5 \times 10^5$ K, below which the cooling becomes exponentially rapid and out of pressure equilibrium. As the pressure drops in the middle, a compression wave moves in. The infalling flow accelerates up to $\sim 0.5 c_h$, moves to the center and then bounces back as an *accretion shock*. In the plane-parallel case, the accretion shock smoothes out the pressure gradient leading to near equilibrium with the background pressure. In the spherical case, on the other hand, the pressure of the shocked gas increases beyond the initial value owing to the central focusing. Thus the density enhancement factor can be as high as 10^6 ($n_h \sim 10^4\ \mathrm{cm}^{-3}$), which is $\sim 10^{3.5}$ higher than the isobaric compression ratio. Although there is a large positive pressure gradient between the cloud core and the background gas, there exists a halo of supersonic accretion flow instead of the out-flow, because the high density and high pressure core is gravitationally bound.

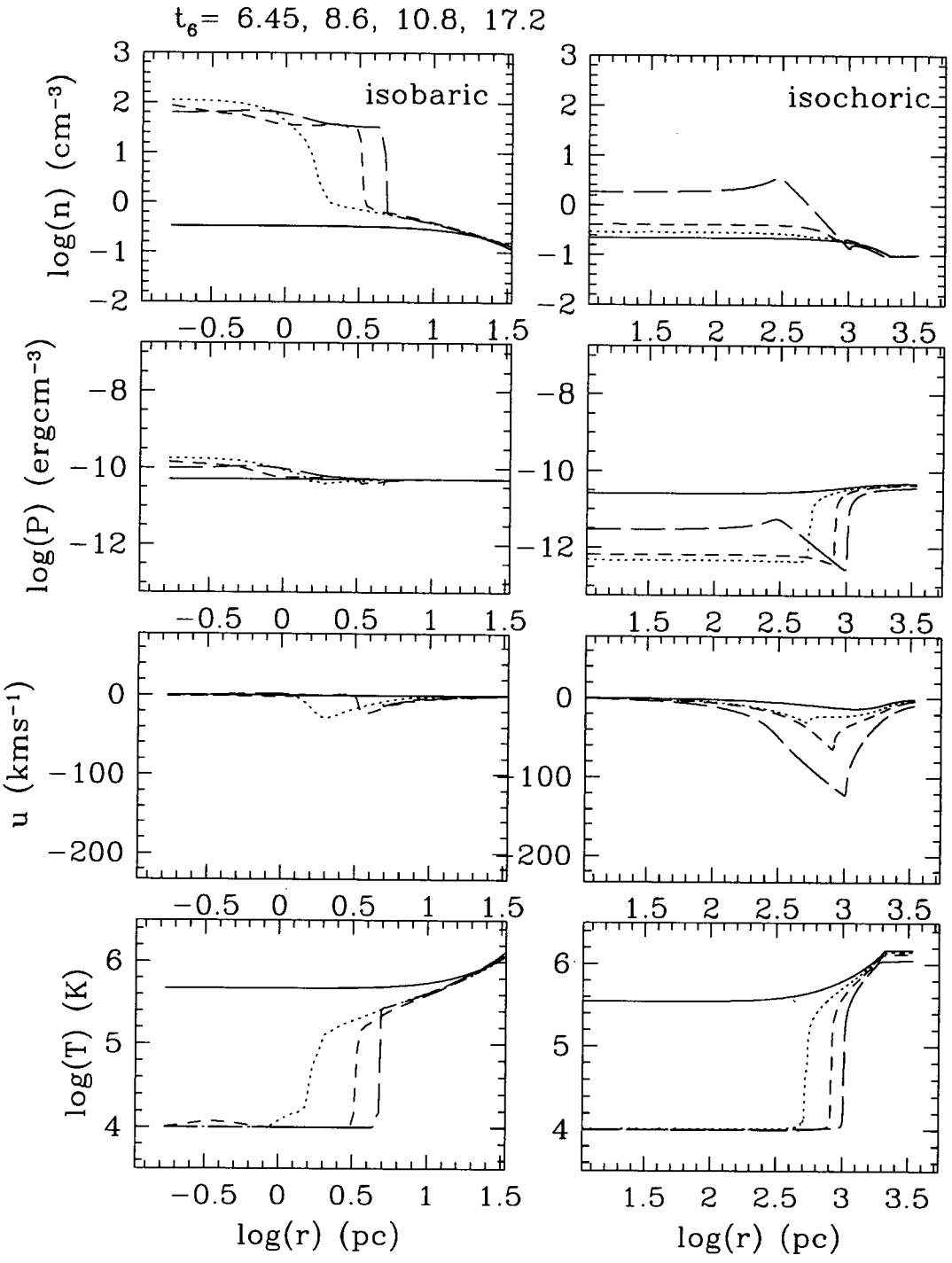

Fig. 2.— Evolution of small *isobaric* (model SM1: $R_c = 0.04 l_{cool}$, left panels) and large *isochoric* (model SM7: $R_c = 2.1 l_{cool}$, right panels) perturbations in one-dimensional spherical geometry. Number density, pressure, radial velocity and temperature are plotted against radius. The background medium has $n_h = 0.1$ cm^{-3} and $T_h = 1.7 \times 10^6$ K. The structure is shown at $t_6 = 6.45$ (solid), 8.6 (dotted), 10.8 (dashed), and 17.2 (long dashed), where t_6 is time in units of 10^6 yrs. The small cloud is compressed isobarically with subsonic flow motions (no shock), while the large cloud cools with only little bit of compression.

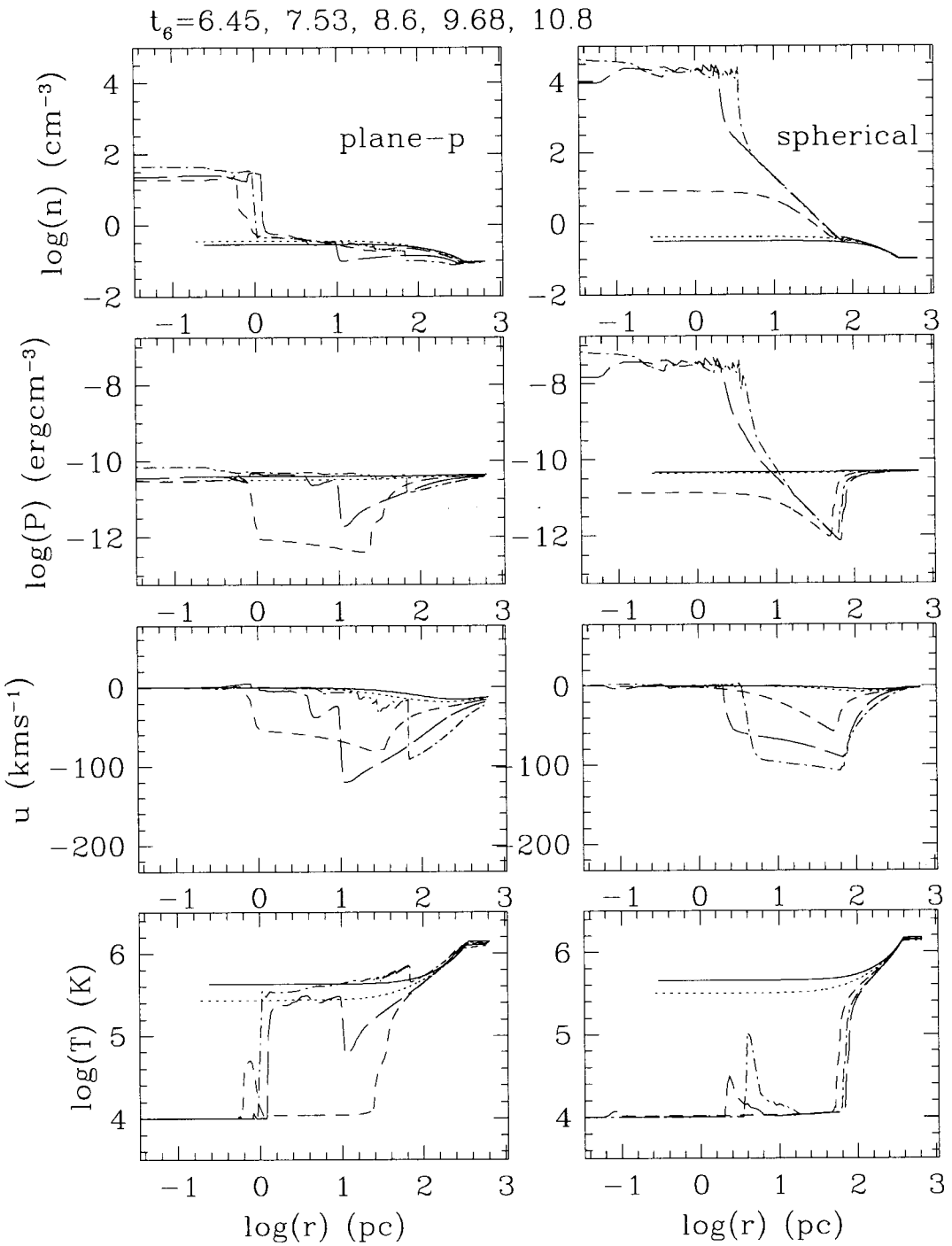

Fig. 3.— Number density, pressure, radial velocity and temperature are plotted against radius for an *intermediate* perturbation of $R_c = 0.4 l_{cool}$ in a background medium of n_h = 0.1 cm^{-3} and $T_h = 1.7 \times 10^6$ K. The panels on the left are for one-dimensional plane-parallel geometry, while those on the right are for one-dimensional spherical geometry. The structure is shown at $t_6 = 6.45$ (solid), 7.53 (dotted), 8.6 (dashed), 9.68 (long dashed) and 10.8 (dot-dashed), where t_6 is time in units of 10^6 yrs.

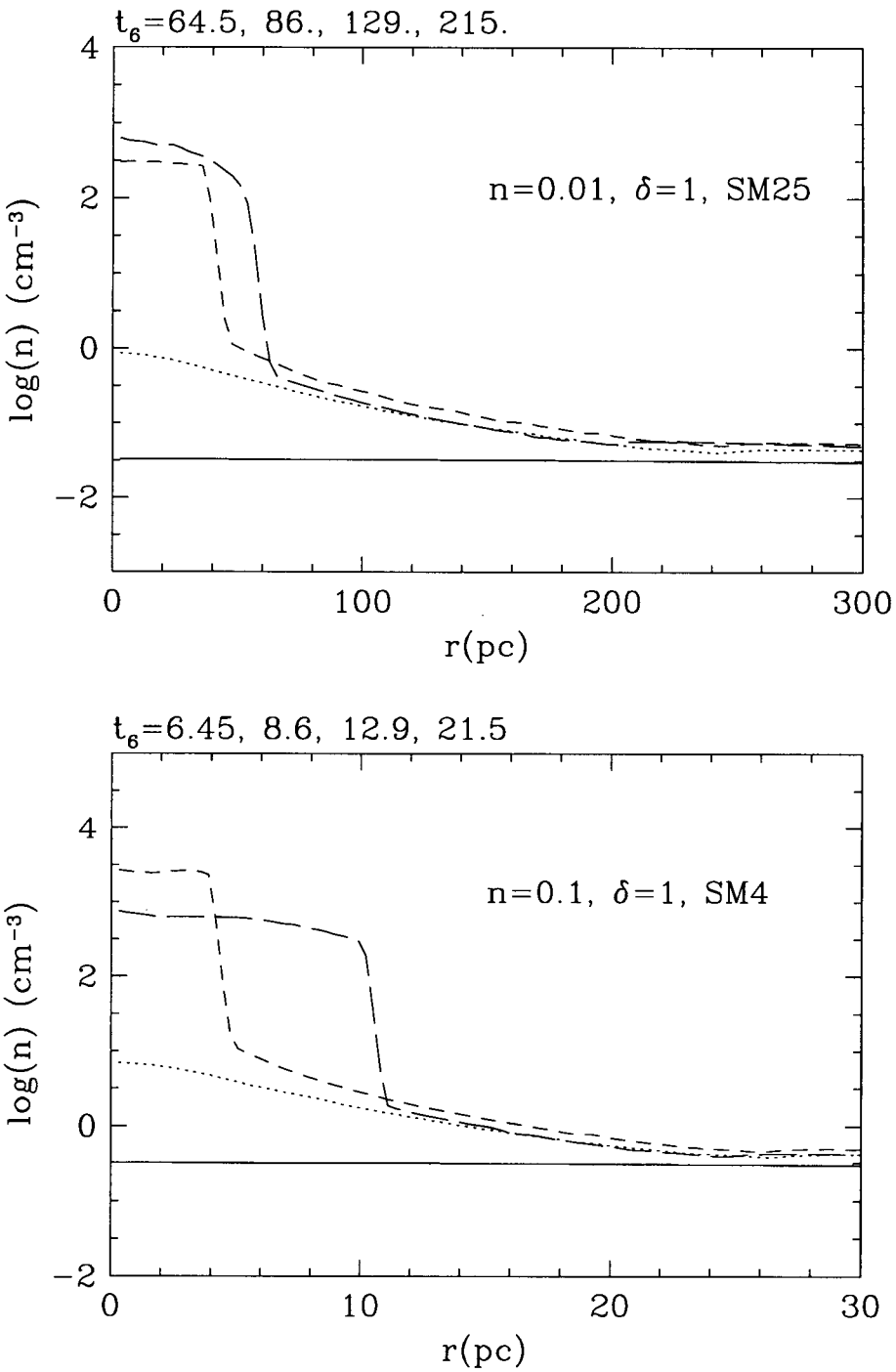

Fig. 4.— Density profiles of PGCCs are plotted for models SM25 and SM4 at $t_6(n_h/0.1\ \mathrm{cm}^{-3}) = 6.45$ (solid), 8.6 (dotted), 12.9 (dashed), and 21.5 (long dashed), where t_6 is time in units of 10^6 years. They can be characterized by a core plus a r^{-2} halo.

Fig. 4 shows the density profiles of the clouds of *intermediate* size ($R_c \sim 0.42 l_{cool}$) with different halo densities, SM25 ($n_h = 0.01$ cm^{-3}) and SM4 ($n_h = 0.1$ cm^{-3}). This suggests that the density profiles of PGCCs can be represented by a core with a halo of $\rho \propto r^{-2}$. Since the gravitational time scale decreases with the density as $n^{-1/2}$ while the cooling time scale decreases as n^{-1}, the relative importance of self-gravity increases in lower density models. For example, the model SM25 stops expanding after $t_6 \sim 215$, while the cloud in SM4 expand outward slowly. But the expansion speed is about 0.7 km s^{-1}, much less than the sound speed of 10^4 K gas.

Vietri & Pesce (1995) proposed that, instead of the quasi-static evolution into the two-phase medium, overdense regions create an implosion shock that leads to H_2 formation and cooling of the post-shock gas to 10^2 K (assuming no external UV radiation). However, we found that the implosion shock develops only if the initial density perturbation is strongly nonlinear ($\delta >> 1$) or has a discontinuous top-hat distribution, both of which are unlikely in real density perturbations. Even in these cases, the implosion shock is nearly isothermal due to the rapid cooling of the post-shock gas. When the implosion shock rebounds at the center, it becomes an accretion shock. The post accretion shock gas still cools rapidly and condenses, so Vietri & Pesce's "small dispersing clouds" are an artifact of their methods.

(b) Physical Properties of PGCCs

According to our numerical calculations, only the intermediate size clouds in the supersonic compression regime, that is, 0.4 kpc $\lesssim R_c(n_h/0.05$ cm$^{-3}) \lesssim 2$ kpc and $10^{5.6}$ M$_\odot \lesssim M_c(n_h/0.05$ cm$^{-3})^2 \lesssim 10^8$ M$_\odot$, become PGCCs via thermal instability. Smaller clouds in the isobaric limit are not gravitationally bound (see in next subsection), while bigger clouds in the isochoric limit are too large to outrace the evolution of the background gas to become distinct structures. The relevant cloud sizes increase for lower halo gas densities (so for greater R_g), since the cooling distance is inversely proportional to the gas density. But the formation time becomes longer at lower densities and the length scale increases to a scale on which other dynamical effects may suppress the density growth.

In the transition from *small* to *intermediate* clouds, we see larger compressions owing to the supersonic infall with the compression factor increasing with the mass of the cloud (see Figs. 1 and 2). Thus the final radii of PGCCs, R_{pgcc}, lie in the narrow range: R_{pgcc} $(n_h/0.05$ cm$^{-3}) \sim 30 - 60$ pc. This owes to the dynamics of the supersonic infall whereby the shock in a larger cloud has a greater opportunity to accelerate and contributes more to its overall compression. This is extremely interesting, as the half mass radii of globular clusters varies by only about a factor of ~ 3 over two decades in mass (*c.f.* Fall & Rees 1977).

PGCCs form within $2t_{cl,c} \approx (2 \times 10^7$ yrs) (0.05 cm^{-3} $/n_h)$, while the background halo gas cools in a time scale of $2t_{cl,h} \approx (8 \times 10^7$ yrs)(0.05 cm$^{-3}/n_h)$. So PGCCs would lose the background pressure support in the same time scale, unless the halo gas is continuously heated by stellar winds and supernova explosion from Pop III stars or accretion shocks or shocks generated by merging sub-clumps. Thus only self-binding *intermediate* clouds keep their identity, while clouds disperse.

(c) Fragmentation of PGCCs

Although our numerical simulations are limited to one dimension and cannot follow the thermal history of PGGCs below 10^4 K, we expect the dense core of PGCCs may fragment further owing to self-gravity. If the shape of PGCCs is more like a pancake, then the cloud would break up first by other dynamical instabilities into more or less spherical fragments and then only gravitationally unstable fragments undergo further collapses. Thus it is beyond our study to make the detail predictions on fragmentation processes. Here we attempt to make a rough estimate of the minimum mass scale of unstable PGCCs.

For small isobaric clouds with $M_c < 10^{5.6}$ M$_\odot$ $(n_h/0.05$ cm$^{-3})^{-2}$, the minimum unstable mass can be the "critical mass", M_{cr} adopted by FR85, which was derived for an isothermal sphere confined by an external pressure (McCrea 1957),

$$M_{cr} = 1.18 \left(\frac{kT_c}{\mu m_H}\right)^2 G^{-3/2} p_h^{-1/2} \qquad (14)$$

For $T_c = 10^4$ K and $p_h = 1.17 \times 10^{-11}$dyne cm^{-2}, $M_{cr} \sim 4.7 \times 10^6$ M$_\odot > M_{small}$, so the small clouds are too small to become unstable gravitationally.

For intermediate size clouds, as shown in Figs. 3-4 (spherical cases), the density distribution of a typical PGCC can be approximated by a dense core with a halo of $\rho \propto r^{-2}$. The flow in the core is almost static while the outer region is infalling supersonically. Thus the core of PGCCs can be approximated by an almost uniform static sphere. This is certainly different from the singular isothermal distribution ($\rho \propto r^{-2}$ all the way to $r = 0$), which is often assumed in the previous studies mentioned in the introduction. In this case, PGCCs are confined by self-gravity and the background pressure is negligible, so M_{cr} given in Eq. (14) is not relevant. In a simple approach where the virial equilibrium is used (McCrea 1957) (*e.g.*, $2K + \Omega \approx 0$, where $2K = 3MkT/(\mu m_H)$ is the thermal energy and $\Omega = -(3/5)GM^2/R$ is the gravitational potential energy for a uniform sphere), the minimum unstable mass is given by

$$M_{vir} = 5.46 \left(\frac{kT_c}{\mu m_H G}\right)^{3/2} {\rho_c}^{-1/2}, \qquad (15)$$

where T_c and ρ_c are the temperature and density of condensed PGCCs. In fact this mass scale is almost the

same as Jeans mass of the isothermal uniform sphere (Spitzer 1979) defined as

$$M_J = \rho\lambda_J^3 = 5.57\left(\frac{kT_c}{\mu m_H G}\right)^{3/2}\rho_c{}^{-1/2}. \quad (16)$$

Thus we take this definition of Jeans mass as the minimum mass of unstable PGCCs as $M_J \sim (5.9 \times 10^6\ \mathrm{M}_\odot)T_4^{3/2}n_2^{-1/2}$ where $T_4 = T_c/10^4$ K and $n_2 = n_c/(100\ \mathrm{cm}^{-3})$. Thus supersonic compression lowers the Jeans mass by the square root of the additional compression factor. Owing to the spherical convergence, the highest compression factor we have seen in our numerical simulation is 10^6, up to $\sim 10^{3.5}$ times higher than the isobaric compression. For PGCCs considered here, $0.1 \lesssim n_2 \lesssim 100$, so the Jeans mass in the *intermediate* clouds is $10^{5.5}\ \mathrm{M}_\odot \lesssim M_J(n_h/0.05\ \mathrm{cm}^{-3})^{1/2} \lesssim 10^{7.2}\ \mathrm{M}_\odot$. Considering that the critical star formation efficiency may range between 0.1 and 0.5 in order for the resulting cluster to be self-bounded (Elmegreen *et al.* 1999), this Jean mass scale can be consistent with the observed GC mass distribution. If the evolution of more realistic clouds leads to irregular pancake-like shapes (§2.2, BMM90), however, the density enhancement for real clouds would be smaller than what is found in the spherical simulations, but still larger than the isobaric compression.

The use of shocks to lower the Jeans mass to a value that is closer to the characteristic mass of GCs was considered by Gunn (1980) in the context of chaotic protogalactic collapse and by Lake (1987) who invoked shocks created by cloud-cloud collisions. The cases considered by Gunn and Lake both have so much shear that they would be unlikely to lead to bound structures, but shocks generic to the collapse of the *intermediate* mass clouds don't have this problem and still serve to reduce the Jeans mass to a value that is characteristic of GCs.

IV. CONCLUSION

We re-examined Fall & Rees (1985) model for the formation of PGCCs via thermal instabilities by numerical simulations of overdense clouds in a protogalactic halo. The key idea of this model is that characteristic mass scale of GCs, $M_c \sim 10^6\ \mathrm{M}_\odot$, can be explained by imprinting of critical (Jeans) mass of gas cloud at 10^4 K which has cooled from a hot halo gas in pressure equilibrium via thermal instability. If there were significant cooling below 10^4 K due to H_2 and metals, the cloud will continue to cool and the imprinting is not possible (Kang et al 1990). Then the model fails. So we considered the cases where the radiative cooling is ineffective below 10^4 K, because the formation of H_2 molecules is delayed due to UV radiation from a central AGN or diffuse radiation from halo gas.

The main conclusions are summarized as follows:

1. Unlike X-ray cluster cooling flows, a protogalactic halo provides much more favorable conditions for thermal instability to operate. So PGCCs can form from marginally nonlinear (*i.e.* $\delta \gtrsim 1$) density inhomogeneities in a protogalactic halo via thermal instability. Linear perturbations are likely to be disrupted by the buoyancy-driven instabilities (Balbus & Soker 1989; Reale *et al.* 1991).
2. The size of thermally unstable perturbations is determined by the cooling distance, l_{cool}, over which a sound wave can travel in a cooling time. According to our numerical simulations in one-dimensional spherical geometry, the clouds of $0.2\ l_{cool} \lesssim R_c \lesssim l_{cool}$ can condense to form PGCCs via thermal instability. Smaller clouds ($R_c \lesssim 0.2 l_{cool}$) cool only *isobarically* and become gravitationally unbound clouds, while larger cloud ($R_c \gtrsim l_{cool}$) cool *isochorically* and so do not condense to form any distinct structures.
3. The thermally unstable clouds, which have mass $10^{5.5}\ \mathrm{M}_\odot \lesssim M_{PGCC}(n_h/0.05\ \mathrm{cm}^{-3})^2 \lesssim 10^8\ \mathrm{M}_\odot$, are compressed supersonically, and the density enhancement of $10^3 - 10^6$ results. This is much higher than what is expected from an isobaric compression. Considering the larger compression factor, we estimate the Jeans mass for PGCCs as $10^{5.5}\ \mathrm{M}_\odot \lesssim M_J(n_h/0.05\ \mathrm{cm}^{-3})^{1/2} \lesssim 10^{7.2}\ \mathrm{M}_\odot$. The density distribution of simulated PGGCs can be approximated by an isothermal distribution with a constant core.

Although we focus on the formation of old halo GCs in the Milky Way in this work, we note globular clusters exist in some extremely different systems. The largest of the dwarf spheroidals, Fornax, Sagittarius, NGC 147, NGC 185 and NGC 205 all possess GCs. The specific frequency of clusters in these dwarf systems is as large as in bright ellipticals and larger than in spirals (Hodge 1988). If gas were in hydrostatic equilibrium in these parent galaxies, the temperature would be just $10^4 - 10^5$K. Thus a different model other than thermal instability model for the formation of PGCCs or the formation of GCs themselves is necessary for these systems.

Many models for GC formation have been suggested so far, but none of them seem to be complete or can explain all the observed properties of GCs. One of the aspects of FR85 model that has not been touched upon in the present work is the effect of the turbulent motions in the halo. Turbulent energy equivalent to the virial temperature should be injected at the largest scale and cascade down to smaller scales. According to 2D simulations by Vázquez-Semadeni, Gazol, & Scalo (2000) the turbulence cannot suppress the thermal instability, because the time scale for the thermal instability remains shorter than the turbulent crossing time scale ($R_{\mathrm{cloud}}/v_{\mathrm{turb}}$) at smaller scales than the virialization-scale. This is because the turbulent velocity decreases faster than the scale, so the turbulent crossing time

increases at smaller scales. On the other hand, the turbulence can provide some heating to the halo gas. Since the halo gas cools radiatively in about 10^8 yrs, additional heating is necessary to maintain the halo temperature at T_h for much longer than the cooling time scale in order to explain the observed age spread of GCs, typically a few Gyr.

As discussed in §2, it is necessary to consider more realistic multi-dimensional simulations of thermally unstable clouds in a protogalactic halo environment, which is currently under study. The present work, based on one-dimensional considerations, however, provides useful guidance for the up-coming multi-dimensional works.

The work by HK was supported in part by Pusan National University Research Grant, 1999. The work by GL was supported in part by NASA HPCC/ESS, ATP and LTSA at the University of Washington. The work by HK and DR was supported in part by grant 1999-2-113-001-5 from the interdisciplinary research program of the KOSEF. HK and DR acknowledge generous hospitality by the University of Washington, while this work had been carried out.

REFERENCES

Ashman, K. M. & Zepf, S. E. 1992, ApJ, 384, 50.

Balbus, S. A. 1986, ApJL, 303, L79.

Balbus, S. A. & Soker, N. 1989, ApJ, 341, 611.

Brinkmann, W., Massaglia, S. & Müller, E. 1990, A&A, 237, 536 (BMM90).

Brown, J. H., Burkert, A. & Truran, J. W. 1991, ApJ, 376, 115.

Colella, P. & Woodward, P. R. 1984, J. Comp. Phys., 54, 174.

David, L. P., Bregman, J. N. & Seab, C. G. 1988, ApJ, 329, 66 (DBS88).

Dopita, M. A. & Smith, G. H. 1986, ApJ, 304, 283 .

Elmegreen, B. G., Efremov, Y. N., Pudritz, R. E., & Zinnecker, H., 1999, astro-ph/9903136

Fall, S. M. & Rees, M. J. 1977, MNRAS, 181, 37.

Fall, S. M. & Rees, M. J. 1985, ApJ, 298, 18.

Gray, D. R. & Kilkenny, J. D., 1980, Plasma Phys., 22, 81.

Gunn, J.E. 1980, in *Globular Clusters*, ed. D. Hanes & G. Madore, (Cambridge: Cambridge University Press), p. 301.

Hattori, M. & Habe, A. 1990, MNRAS, 242, 399.

Hodge, P. 1988, PASP, 100, 568.

Kang, H., Shapiro, P. R., Fall, S. M. & Rees, M. J. 1990, ApJ, 363, 488.

Kumai, Y., Baku, B. & Fujimoto, M. 1993, ApJ, 404, 144.

Lake, G. 1987, in *IAU Symposium 127, Structure and Dynamics of Elliptical Galaxies*, ed. T. de Zeeuw, (Dordrecht: Reidel), p. 331.

Malagoli, A., Rosner, R. & Bodo, G. 1987, ApJ, 319, 632.

Malagoli, A., Rosner, R. & Fryxell, B. 1990, MNRAS, 247, 367.

McCrea, W. H. 1957, MNRAS, 117, 562.

Reale, F., Rosner, R., Malagoli, A., Peres, G. & Serio, S. 1991, MNRAS, 251, 379.

Shapiro, P. R. & Kang, H. 1987, ApJ, 318, 32.

Spitzer, L. 1979, Physical Processes in the Interstellar Medium, (New York: Wiley-Interscience).

Vázquez-Semadeni, E., Gazol, A., & Scalo, J., 2000, astro-ph/0001027

Vietri, M. & Pesce, E. 1995, ApJ, 442, 618.

Yoshida, T., Hattori, M. & Habe, A. 1991, MNRAS, 248, 630.

Zinn, R. 1985, ApJ, 392, 424.